Effect of Peptide Lipidation on Membrane Perturbing Activity: A Comparative Study on Two Trichogin Analogues

Emanuela Gatto,[†] Claudia Mazzuca,[†] Lorenzo Stella,[†] Mariano Venanzi,[†] Claudio Toniolo,[‡] and Basilio Pispisa*[,†]

Dipartimento di Scienze e Tecnologie Chimiche, Università di Roma Tor Vergata, 00133 Roma, Italy, and Dipartimento di Scienze Chimiche, Università di Padova, 35131 Padova, Italy

Received: July 19, 2006; In Final Form: September 5, 2006

The effect of lipidation on the membrane perturbing activity of peptaibol antibiotics was investigated by performing a comparative study on two synthetic analogues of the natural peptide trichogin GA IV. Both analogues were labeled with a hydrophobic fluorescent probe, but one of them lacked the N-terminal *n*-octanoyl chain, present in the natural peptide. Spectroscopic studies show that the fatty acyl chain produces two opposite effects: it increases the affinity of the monomeric peptide for the membrane phase, but, at the same time, it favors peptide aggregation in water, thus inhibiting membrane binding by reducing the effective monomer concentration. In the membrane phase the two analogues exhibit the same aggregation and orientation behavior, indicating that the *n*-octanoyl chain plays no specific role in determining their orientation or membrane perturbing activity. Indeed, the dependence of peptide-induced membrane leakage on total peptide concentration is basically the same for the two analogues, because the aforementioned opposite effects, caused by peptide lipidation, tend to balance. These findings make questionable the use of lipidation as a *general* method for increasing the peptide membrane-perturbing activity, as its validity seems to be restricted to parent compounds of limited overall hydrophobicity.

Introduction

Antibiotic peptides represent a fundamental component of the innate defense system of all organisms, killing pathogens by making their cell membrane permeable.[1−3] Despite the large number of studies, the molecular details of the activity of these peptides are still being debated.[4]

Recently, we have determined several features of the mechanism of pore formation by the antibiotic peptide trichogin GA IV.[5,6] This peptide belongs to the family of lipopeptaibols,[7] and has the following primary structure:

n-Oct-Aib[1]-Gly[2]-Leu[3]-Aib[4]-Gly[5]-Gly[6]-Leu[7]-Aib[8]-Gly[9]-Ile[10]-Lol

where *n*-Oct is *n*-octanoyl, Aib is α-aminoisobutyric acid, and Lol is leucinol.[8,9] We proved that trichogin forms aggregates both in water and in the membrane, and that membrane perturbation arises from the aggregates formed in the lipid bilayer. By contrast, aggregation in water affects the final activity only because it inihibits peptide binding to the membrane, by reducing the effective monomer concentration. Below a threshold concentration trichogin binds to the membrane surface in the monomeric form. As the membrane-bound peptide concentration increases, a cooperative transition occurs, leading to peptide insertion into the lipid bilayer and formation of aggregates. These oligomers constitute the pores causing membrane leakage and bioactivity,[6] a behavior reminiscent of the "two-state model" proposed by Huang and co-workers.[10,11] However, some fundamental aspects of the mechanism of action of trichogin, such as the structure of the pores and the function of specific residues, need further investigation. The aim of the present work is primarily that of clarifying the role of the *n*-octanoyl chain in the membrane-perturbing mechanism of trichogin.

Lipidation of bioactive peptides has been proposed as a way to increase their membrane binding tendency and biological activity.[12−14] However, the ultimate effect of an acyl chain on the overall membrane activity of an antibiotic peptide is difficult to predict, as illustrated by studies on trichogin analogues having acyl chains of different length.[15] The membrane-perturbing activity increases up to a chain length of 10 carbon atoms, but a further elongation of the aliphatic chain causes a decrease in activity. On the other hand, trichogin analogues in which the acyl chain is shorter than five carbon atoms are completely inactive, a finding suggestive of a fundamental role of the acyl chain in determining both the position and orientation of trichogin in the membrane and formation of pores, even though the long acyl chain can be moved to different positions along the peptide chain without significant loss of activity.[16]

To shed further light on these points, we investigated two synthetic fluorescent trichogin analogues (F10 and F0). The fluorenyl-based fluorescent label in F10 was introduced into the side chain at position 10 and in F0 it replaced the N-terminal *n*-octanoyl moiety, as shown below:

n-Oct-Aib-Gly-Leu-Aib-Gly-Gly-Leu-Aib-Gly-Dab(Fmc)-Leu-OMe (F10)

Fmoc-Aib-Gly-Leu-Aib-Gly-Gly-Leu-Aib-Gly-Ile-Leu-OMe (F0)

where Fmc is fluorenyl-9-methylcarbonyl, Fmoc is fluorenyl-9-methyloxycarbonyl, Dab is 2,4-diaminobutyric acid, and OMe

* To whom correspondence should be addressed. E-mail: pispisa@stc.uniroma2.it.
[†] Università di Roma Tor Vergata.
[‡] Università di Padova.

10.1021/jp064580j CCC: $33.50
Published on Web 10/18/2006

is methoxy. This study was motivated by the unexpected observation that these analogues, notwithstanding the significant differences in their primary sequences, exhibit very similar membrane perturbing activities, as shown below. Preliminary spectroscopic data on the analogue F10 recently have been reported,[5] but a detailed comparison between the membrane activities of the two analogues, together with a thorough analysis of their aggregation and partition behavior, are presented here. They provide a deeper understanding of the membrane-perturbing activity of trichogin and of the role of the *n*-octanoyl moiety.

Experimental Section

Materials. Phospholipids were purchased from Avanti Polar Lipids (Alabaster, AL) and carboxyfluorescein and Sephadex G-50 from Sigma (St. Louis, MO). Spectroscopic grade chloroform and methanol (C. Erba, Milan, Italy) were used. Poly(vinyl alcohol) (PVA), average MW 22 000, 88% hydrolyzed, and Triton X-100 were Acros (Geel, Belgium) products.

Peptide Synthesis. Peptide syntheses were carried out in solution, using the segment condensation approach. Peptide coupling reactions were performed by either the [1-(3-dimethylamino)propyl]-3-ethylcarbodiimide (EDC)/(1-hydroxy-1,2,3-benzotriazole)[17] or by the EDC/(7-aza-1-hydroxy-1,2,3-benzotriazole) HOAt method.[18] In F10, the Fmc group was introduced into the Dab side chain of the C-terminal octapeptide intermediate by using EDC/HOAt. Details of the syntheses and characterizations of peptides F0 and F10 and their synthetic intermediates are reported in ref 19.

Liposome Preparation. Large unilamellar vesicles (LUVs) were prepared by dissolving lipids in a $CHCl_3$/MeOH solution (1:1, v/v). The solvents were evaporated under reduced argon atmosphere, until a thin film formed. Complete evaporation was ensured by applying a rotary vacuum pump for at least 2 h. The film was hydrated with a 20 mM Tris buffer (pH 7.0), containing 140 mM NaCl and 1 mM EDTA, whereas for release experiments a 30 mM carboxyfluorescein solution was used. After vigorous stirring and 10 freeze and thaw cycles, the liposome suspension was extruded 31 times through two stacked polycarbonate membranes with 100 nm pores (Avestin, Ottawa, ON, Canada). For release experiments, the unencapsulated fluorescent tracer was separated from the liposomes by gel filtration on a Sephadex G-50 medium column. Final phospholipid concentration was determined by the Stewart method.[20] All liposomes were formed by egg phosphatidylcholine (ePC) and cholesterol (1:1 molar ratio).

Liposome Leakage. Peptide-induced membrane permeability was determined by measuring the fractional release of carboxyfluorescein entrapped into the liposomes, following the increase in fluorescence intensity (excitation 490 nm, emission 520 nm) caused by the reduction in self-quenching.[21] Peptides were added to water solutions from small aliquots of a concentrated MeOH solution, in such a way that the MeOH amount in the final sample was always less than 1%. Control experiments performed by adding MeOH to carboxyfluorescein loaded vesicles clearly show that this small amount of organic solvent does not cause any membrane perturbation, as indicated by the lack of any vesicle leakage.

Fluorescence Quenching. Iodide quenching experiments were performed by titrating a 2 mM vesicle solution, containing 1 μM of the fluorescent peptide analogue, with aliquots of a solution containing 4 M KI and 1 mM Na_2SO_3, prepared on the same day. Solutions were excited at 280 nm and emission was measured at 304 nm. Quenching of the analogues in the absence of liposomes was also measured for comparison.

Depth-Dependent Quenching. The degree of labeling of doxyl-containing lipids [(1-palmitoyl-2-stearoyl(*n*-doxyl)-*sn*-glycero-3-phosphocholine] was determined by double integration of EPR spectra.[22] Doxyl-labeled liposomes were produced by adding the labeled lipids to the initial $CHCl_3$ solution (7% molar fraction). Spin label content was also controlled directly on the final liposomes by double integration of the EPR spectra of an aliquot of the liposomes dissolved in 2-propanol. All liposome preparations contained the same amount of spin labels, within a 10% error. The fluorescent peptide analogues were added to the different doxyl-labeled liposomes (at a lipid concentration of 0.2 or 2 mM) and to a reference unlabeled liposome solution. Steady-state fluorescence intensities were determined after a 20 min equilibration period.

CD and Fluorescence Spectroscopy. CD spectra were recorded with a J-600 Jasco apparatus (Tokyo, Japan) with appropriate quartz cells. Steady-state fluorescence spectra were measured on a SPEX Fluoromax fluorimeter (Edison, NJ). Time-resolved experiments were performed on a CD900 single photon counting apparatus (Edinburgh Instruments, Edinburgh, U.K.). Nanosecond pulsed excitation was obtained with a flash-lamp filled with ultrapure hydrogen (0.3 bar, 40 kHz repetition rate; full width at half-maximum 1.2 ns). Fluorescence intensity decays were acquired until a peak value of 10^4 counts was reached and analyzed with the software provided by Edinburgh Instruments. Temperature was controlled within ± 0.1 °C with a thermostated cuvette holder. The fluorene chromophores were excited at 265 nm, and time-resolved fluorescence decays were acquired by collecting emission at 315 nm, with a bandwidth of 20 nm and a WG305 cutoff filter. Water−membrane partition experiments were performed by using $\lambda_{exc} = 288$ nm and $\lambda_{em} = 330$ nm, and correcting intensities for scattering effects,[23] using tryptophan as a reference.

To minimize peptide adsorption on cell walls, UV-grade poly(methyl methacrylate) cuvettes were treated overnight with a 5% (w/w) water solution of poly(vinyl alcohol).[24]

Results

Peptide Conformation. In Figure 1 the far-UV CD spectra of the two fluorescent analogues in MeOH solution are compared with that of the unlabeled parent peptide Tric-OMe, a synthetic trichogin analogue with a leucine methyl ester residue at the C-terminus replacing Lol. Extensive studies by X-ray crystallography, CD, FTIR, NMR, EPR, and fluorescence spectroscopies have shown that trichogin and Tric-OMe in solution attain a mixed 3_{10}-/α-helical structure with a hinge point corresponding to the two central glycines.[9,15] The similarity of all three spectra suggests that the fluorescent label, located at different positions, does not perturb the overall conformation of the peptide backbone, and that the extrinsic dichroism of the fluorene moiety is of minor significance, if any. Since this chromophore absorbs strongly in the far-UV spectral region,[25] these data indicate that it is not significantly perturbed by the dissymmetric peptide chain, very likely because of the high mobility of the fluorene moiety.

Membrane Activity of the Trichogin Analogues. To determine the membrane-perturbing activity of the two analogues, the peptide-induced leakage of liposome content was measured. A fluorescent tracer (carboxyfluorescein) was entrapped into the liposomes at 30 mM concentration, so that its emission was self-quenched.[21] Release induced by peptide addition caused a dilution of the fluorophore, determining an increase in fluorescence intensity. The emission intensity corresponding to the total release was determined by disrupting

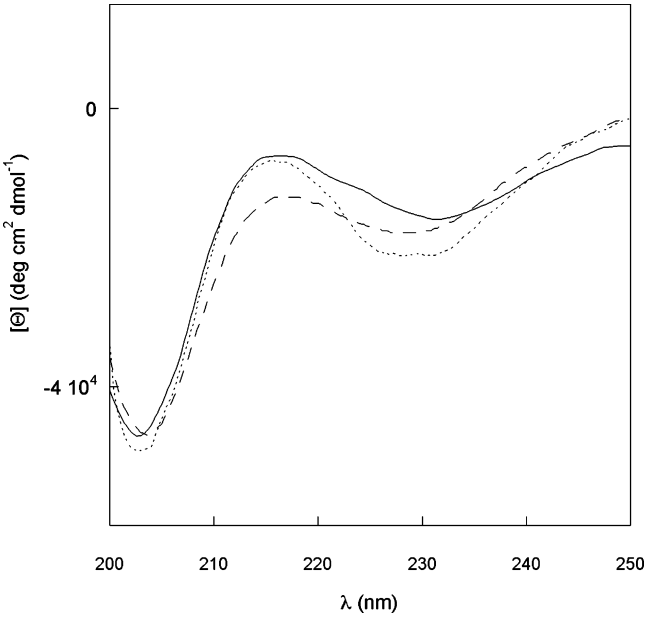

Figure 1. Far-UV CD spectra of analogues F0 (full line) and F10 (dotted line) and of the parent peptide Tric-OMe (dashed line) in MeOH solution. Molar ellipticity refers to total peptide concentration (10^{-4} M).

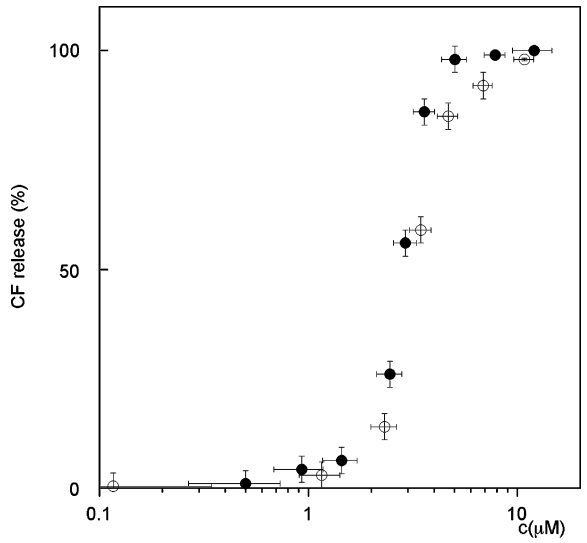

Figure 2. Peptide-induced leakage of carboxyfluorescein (CF) entrapped into ePC/cholesterol liposomes (total lipid concentration: 0.2 mM). Solid symbols, F0; open symbols, F10. Release was determined after 20 min from peptide addition.

the vesicles with the detergent Triton X-100 (final concentration: 1 mM). Figure 2 reports the percentage of liposome content released in 20 min, after peptide addition, as a function of peptide concentration. Surprisingly, despite the structural difference between F0 and F10, the membrane activities of these analogues are very close.

Peptide Aggregation in Water. The fluorescence intensity decay of F0 was measured in water at different peptide concentrations. All these decay data can be fitted globally,[26] by assuming a double exponential function with lifetimes of 6.7 ± 0.1 and 1.6 ± 0.3 ns (global $\chi^2 = 1.0$). This result strongly suggests the presence of two different species, the relative population of which can be determined from the preexponential factors of the two decay components. These populations vary with peptide concentration (Figure 3), indicating the presence of an aggregation equilibrium. The long lifetime component,

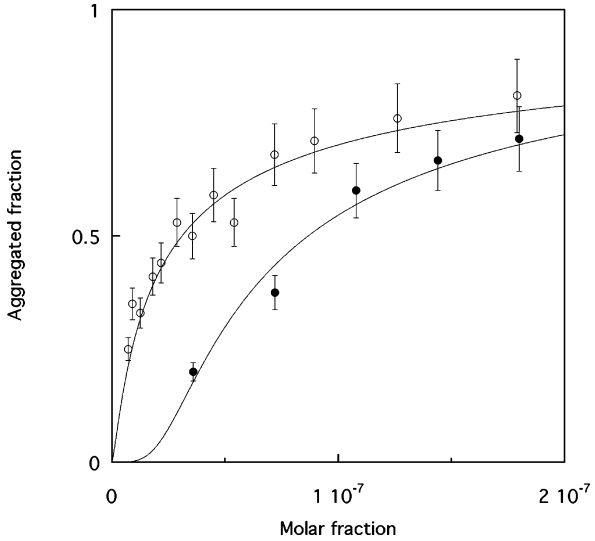

Figure 3. Peptide aggregation in water: fraction of aggregated peptide, as determined from the preexponential factor of the short component of the double exponential fluorescence intensity decay, as a function of peptide concentration. Solid symbols, F0; open symbols, F10.

prevailing at low peptide concentration, very likely corresponds to the monomeric peptide, while the short lifetime can be tentatively assigned to an oligomeric species. The same behavior was observed for F10, with lifetimes of 5.6 ± 0.1 and 0.87 ± 0.08 ns.[5] Figure 3 compares the aggregation curves of the two analogues determined from the fluorescence decay data, showing, not unexpectedly, that F10 aggregates at much lower concentrations than F0, due to the increased hydrophobicity caused by the additional N-terminal *n*-octanoyl moiety.

The relative population data can be fitted assuming that a single aggregate species forms:

$$n\mathrm{M} \rightleftarrows \mathrm{M}_n \qquad (K_\mathrm{A})^{n-1} = \frac{x_{\mathrm{M}_n}}{(x_\mathrm{M})^n}$$

where M indicates the monomeric peptide and *n* the aggregation number.

As a result, the aggregation number and the aggregation constant were $n \approx 2$ and $K_\mathrm{A}^{\mathrm{water}} = (3.4 \pm 0.2) \times 10^7$ for F10 and $n \approx 5$ and $K_\mathrm{A}^{\mathrm{water}} = (1.5 \pm 0.1) \times 10^7$ for F0.

It is noteworthy that the uncertainty in the *n* values is large, because the dependence of the aggregation curves on this parameter is rather weak. In addition, since we have postulated the absence of aggregates of varying size, *n* indicates only a lower limit to the maximum number of peptide chains participating to the oligomeric species.

Membrane−Water Partition. The membrane−water partition of the two analogues was determined by measuring the change in fluorescence intensity caused by the addition of increasing concentrations of liposomes.[27] Figure 4 shows the partition curves measured at three different peptide concentrations (1.1, 11, and 30 μM). In the case of F10, association with the phospholipid bilayer is progressively less favored as the peptide concentration increases. On the other hand, F0 shows a dependence on peptide concentration much less marked than that of the other analogue. However, since a simple partition equilibrium does not depend on peptide concentration,[28] the foregoing data strongly suggest the occurrence of other equilibria, so that the results reported in Figure 4 give rise to apparent partition curves only. If more than one species is present in each phase, having different fluorescence quantum yields, the

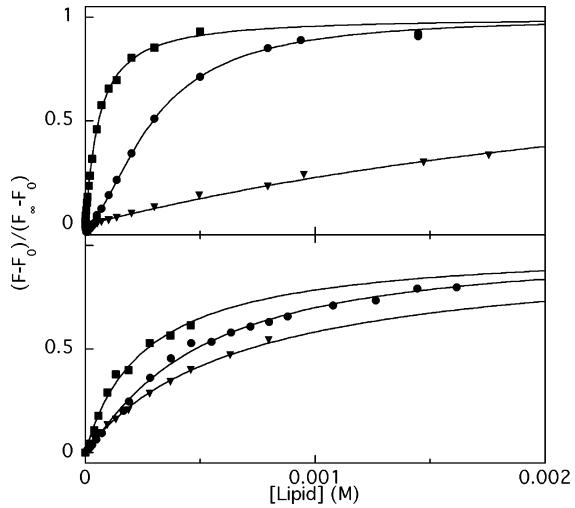

Figure 4. Membrane−water partition curves for F10 (upper panel) and F0 (lower panel), as determined by the increase in peptide fluorescence intensity when a fixed peptide concentration is titrated with increasing amounts of ePC/cholesterol liposomes. Peptide concentration: 1.1 (squares), 11 (circles), and 30 μM (triangles). F_0 is the fluorescence intensity in the absence of liposomes, while F_∞ is the plateau value of fluorescence intensity at very high lipid concentration, extrapolated by a double reciprocal plot.

overall fluorescence intensity depends on the relative concentrations of all species,[29] and, therefore, it is not simply proportional to the fraction of membrane-bound peptide.

In the preceding section we have already shown that both analogues undergo an aggregation equilibrium in water. Formation of aggregates in the membrane phase can be detected by performing the same time-resolved fluorescence experiments in the presence of liposomes. Intensity decays of F0 fluorescence were measured in the presence of liposomes at a total lipid concentration of 2.0 mM and at different peptide concentrations.

The partition curves of Figure 4 indicate that the membrane-bound peptide is in equilibrium with the water phase. Therefore, we expect a very complex fluorescence decay behavior, in which both monomeric and aggregated peptides in water contribute to the overall fluorescence. The lifetimes associated with these components are already known, because they were determined in the absence of liposomes (Figure 3). Therefore, the simplest possible decay model taking into account the peptide remaining in the water phase and that in the membrane is a triple exponential function, with two lifetimes fixed to the values measured in water and the third component corresponding to the membrane-bound peptide. Unfortunately, this fit is not adequate to describe globally all of the experimental decays (global $\chi^2 = 1.9$), indicating that a single component is not sufficient to account for the membrane-bound peptide fraction. As a result, we were forced to assume that at least two different species are also present in the membrane phase. Consequently, a model having two lifetimes for the peptide in the membrane, in addition to those pertaining to the peptide in water, was adopted. By assuming these additional lifetimes as independent of peptide concentration (i.e., "global" parameters), the recovered global χ^2 was 1.0, and the distribution of residuals was very satisfactory (Figure 5). For F0 the two lifetimes associated with the membrane-bound species are 4.9 ± 0.7 and 8.2 ± 0.3 ns. A very similar behavior was observed for the fluorescence decays of F10, with lifetimes associated with the membrane-bound species of 2.2 ± 0.2 and 7.0 ± 0.2 ns.[5] From the preexponential factors of these decay components the aggregation curves for the analogues investigated in the membrane can

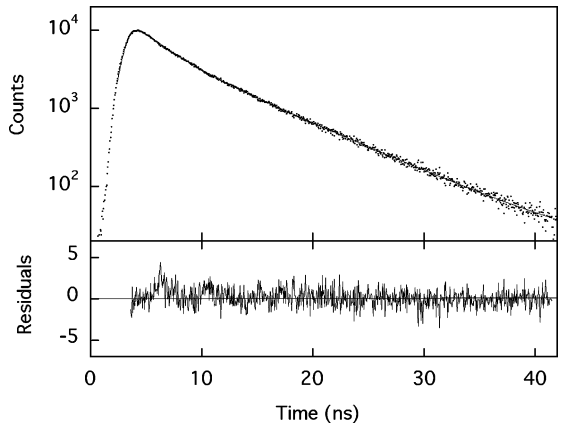

Figure 5. (Upper panel) Fluorescence intensity decay of F0 (50 μM) in the presence of ePC/cholesterol liposomes (2 mM). The solid line represents a fit with the sum of four exponential functions, with two lifetimes fixed to the values observed in the absence of liposomes, and the other two used as global parameters for a fit of the fluorescence decays at eight different peptide concentrations. (Lower panel) Residuals of the four-exponentials fit reported in the upper panel.

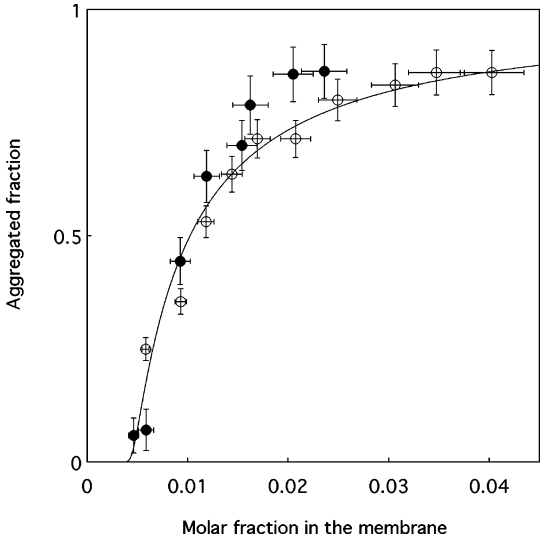

Figure 6. Peptide aggregation in the membrane: the preexponential factors, as determined from a global fit of the time-resolved experiments in the presence of membranes (Figure 5), were used to calculate the fraction of aggregated peptide and of membrane bound peptide. Solid symbols, F0; open symbols, F10.

be obtained, as shown in Figure 6. Within experimental errors, the aggregation behavior of the two analogues in the membrane is undistinguishable, and can be described by a single aggregation curve with $n \approx 25$ and $K_A^{membrane} = 170 \pm 10$. Overall, it can be concluded that the differences observed in the binding curves of the two analogues, reported in Figure 4, are ascribable solely to the different aggregation behavior in water and to the different affinity of the monomers for the membrane.

Peptide Depth and Orientation. We next determined the position and orientation of trichogin with respect to the lipid bilayer, making use of water-soluble and lipid-attached quenchers for fluorescence experiments.

By measuring the efficiency of water-soluble quenchers, it is possible to assess the accessibility of membrane-bound fluorophores from the water phase.[30] Figure 7 illustrates the Stern−Volmer plots corresponding to the iodide quenching of F0 and F10, performed at 1.0 μM peptide concentration and 2 mM lipid concentration. These conditions ensure that the peptides are almost completely bound to the membrane, but at

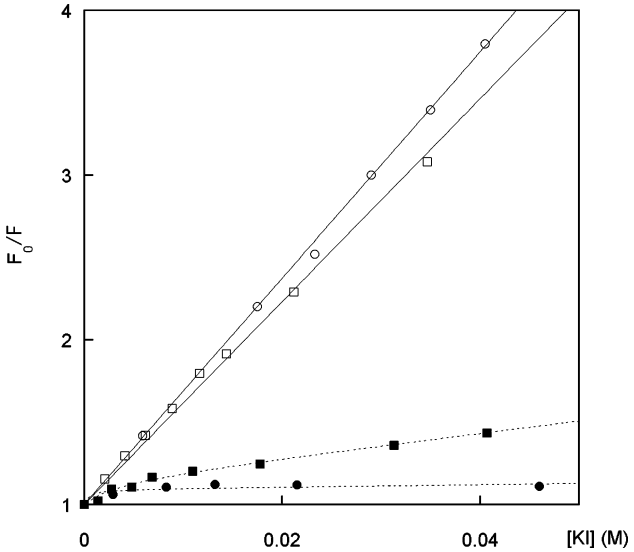

Figure 7. Stern−Volmer plots of iodide-induced quenching of F0 (squares) and F10 (circles) in water (open symbols) and in the presence of liposomes (solid symbols). Lipid concentration: 2 mM. Peptide concentration: 1μM.

this concentration no peptide-induced liposome leakage takes place. For both analogues the quenching caused by iodide ions dissolved in water is significantly reduced by the presence of liposomes, indicating that the peptides are inserted into the membrane, but are still partially accessible to the quencher.

More detailed information on the position of a fluorophore within a membrane can be obtained by the method of depth-dependent quenching,[31,32] in which a quencher covalently bound to the phospholipid acyl chain is exploited. By varying the quencher position along the lipid acyl chain, the immersion depth of a fluorophore within a membrane can be determined, as shown in Figure 8. The quenching measurements were carried out at three different peptide concentrations, i.e., 0.5, 3.5, and 10.8 μM, which correspond to the whole activity range.

At 0.5 μM concentration, the highest decrease in fluorescence intensity is caused by the quenchers located at 7.7 or 10 Å from the bilayer center,[33] i.e., in the region relatively close to the polar headgroups. However, a single distribution does not account for the quenching caused by the lipids labeled in proximity of the bilayer center. On the contrary, a good fit for all experimental data can be obtained by using a double Gaussian depth distribution. This finding clearly indicates that a fraction of the peptide is deeply inserted into the lipid bilayer. As the peptide concentration increases, reaching values high enough to determine liposome leakage, the relative quenching efficiency of the deepest quencher increases significantly, as compared to the efficiency of shallower quenchers. These data suggest the presence of an orientation equilibrium in the membrane, influenced by the ratio between membrane-bound peptide and lipid concentrations (r): at low r values the peptides are located predominantly on the membrane surface, while at high r values (i.e., when the peptide causes liposome leakage) a significant fraction is inserted deeply into the bilayer. Interestingly, a very similar behavior is observed for both F0 and F10, even if the labels are located at the opposite ends in the two analogues, suggesting that the insertion of these peptides into the bilayer can occur indifferently from the N- or the C-terminus.

Conclusions

A close comparison of the behavior of analogues F0 and F10 provides several interesting hints regarding the mechanism of

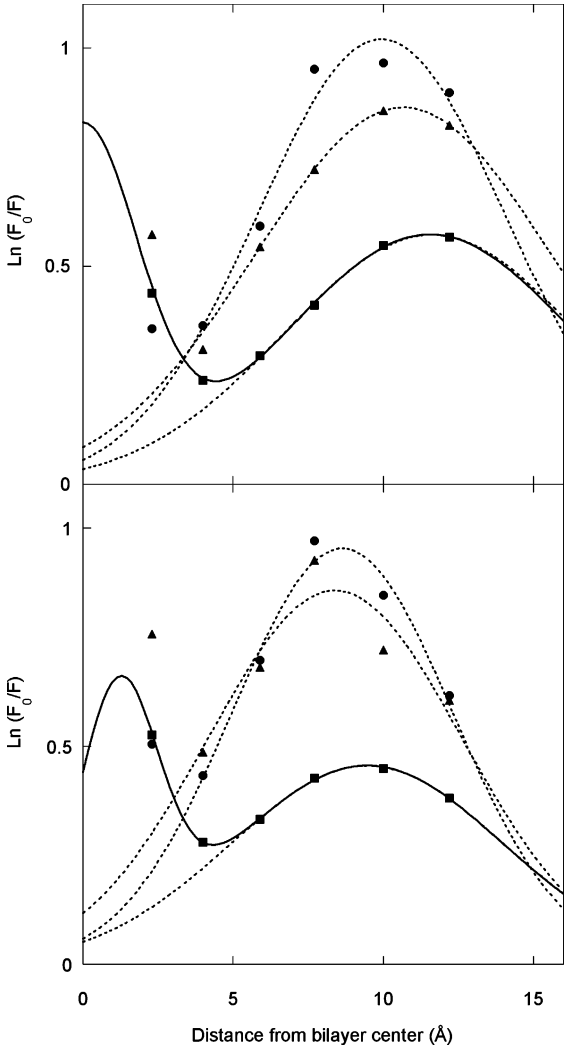

Figure 8. Quenching of the fluorescence intensity (F) of peptides F10 (upper panel) and F0 (lower panel) by phospholipids containing 1-palmitoyl-2-stearoyl(*n*-doxyl)-*sn*-glycero-3-phosphocholine, labeled with a doxyl moiety at different positions along its stearoyl chain. Fluorescence intensities were normalized by the intensity measured in the presence of liposomes not containing labeled lipids (F_0). Peptide concentration: 0.5 (circles), 3.5 (triangles), and 10.8 μM (squares). Lipid concentration: 0.2 mM. $\lambda_{exc} = 290$ nm; $\lambda_{em} = 315$ nm. The data were fitted with a single (broken lines) or double (continuous line) Gaussian distribution. For the sake of clarity, the double Gaussian distribution is reported only for the 10.8 μM data. The abscissa axis refers to the position of the quencher as measured form the center of the bilayer.

pore formation exerted by trichogin. Earlier results have shown that trichogin analogues in which the N-terminal *n*-octanoyl chain is significantly shortened are not membrane active, suggesting that the acyl chain has a fundamental role in the mechanism of membrane perturbation.[15] However, we proved here that analogue F0, in which the acyl chain was substituted by Fmoc, retains the membrane-perturbing activity of the natural peptide. Therefore, it appears that the *n*-octanoyl chain has no specific role, except that of modulating the overall peptide hydrophobicity. This hypothesis is supported by the observation that the long acyl chain can be moved to different positions along the peptide chain without significant loss of activity.[16] Our data provide a clear demonstration of this point: if only the concentration of the membrane-bound peptide is taken into account, the behavior of analogues F0 and F10 in the lipid bilayer is so similar that the data describing their aggregation in the membrane can be fitted by the same curve (Figure 6).

On the other hand, the presence/absence of the acyl chain modifies the hydrophobicity of the peptide, which is reflected in its aggregation and membrane binding behavior. Since F10 aggregates in water at significantly lower concentrations than F0, the corresponding membrane-binding curves are dramatically influenced. At low concentrations (around 1 μM), where both peptides are predominantly monomeric, F10 displays a higher affinity for the lipid bilayer than F0, but as the peptide concentration increases, leading to aggregation in the water phase, the overall binding of F10 to the membrane decreases, while that of F0 is almost unaffected (Figure 4).

This behavior can be described by a simple thermodynamic model, as summarized by the following scheme, where the monomeric peptide partitions between the two phases, and at the same time, aggregation equilibria occur. Obviously, the equilibrium constants and aggregation numbers are different in the two phases.

$$\frac{1}{n}\,\mathrm{M}_n^{\mathrm{W}} \underset{\text{water phase}}{\overset{K_\mathrm{A}^{\mathrm{W}}}{\rightleftharpoons}} \mathrm{M}^{\mathrm{W}} \overset{K_\mathrm{P}}{\rightleftharpoons} \mathrm{M}^{\mathrm{L}} \underset{\text{lipid phase}}{\overset{K_\mathrm{A}^{\mathrm{L}}}{\rightleftharpoons}} \frac{1}{n'}\,\mathrm{M}_{n'}^{\mathrm{L}}$$

In conclusion, the N-terminal *n*-octanoyl chain does not substantially perturb peptide aggregation equilibria in the membrane phase ($K_\mathrm{A}^{\mathrm{L}}$), but it has contrasting effects on the other two equilibria, in the sense that it increases the affinity of the monomeric peptide for the membrane phase (K_P), and at the same time, it enhances peptide aggregation in water ($K_\mathrm{A}^{\mathrm{W}}$), thus reducing the effective monomeric concentration, and hence its binding to the membrane. These two effects almost balance, leading to an overall activity curve very similar for both peptides. Therefore, lipidation should not be considered as a *generally* applicable method to increase the membrane-perturbing activity of antibiotic peptides, even though it could be beneficial when the original peptide is not already strongly hydrophobic.

References and Notes

(1) Zasloff, M. *Nature* **2002**, *415*, 389−395.
(2) Boman, H. G. *J. Intern. Med.* **2003**, *254*, 197−215.
(3) Bulet, P.; Stöcklin, R.; Menin, L. *Immunol. Rev.* **2004**, *198*, 169−184.
(4) Yang, L.; Harroun, T. A.; Weiss, T. M.; Ding, L.; Huang, H. W. *Biophys. J.* **2001**, *81*, 1475−1485.
(5) Stella, L.; Mazzuca, C.; Venanzi, M.; Palleschi A.; Didonè, M.; Formaggio F.; Toniolo C.; Pispisa, B. *Biophys. J.* **2004**, *86*, 936−945.
(6) Mazzuca, C.; Stella, L.; Venanzi, M.; Formaggio, F.; Toniolo, C.; Pispisa, B. *Biophys. J.* **2005**, *88*, 3411−3421.
(7) Toniolo, C.; Crisma, M.; Formaggio F.; Peggion, C.; Epand, R. F.; Epand, R. M. *Cell. Mol. Life Sci.* **2001**, *58*, 1179−1188.
(8) Auvin-Guette, C.; Rebufatt, S.; Prigent, Y.; Bodo, B. *J. Am. Chem. Soc.* **1992**, *114*, 2170−2174.
(9) Peggion, C.; Formaggio, F.; Crisma, M.; Epand, R. F.; Epand, R. M.; Toniolo, C. *J. Pept. Sci.* **2003**, *9*, 679−689.
(10) Huang, H. W.; Chen, F. Y.; Lee, M. T. *Phys. Rev. Lett.* **2004**, *92*, 198304.
(11) Lee, M. T.; Hung, W. C.; Chen, F. Y.; Huang, H. W. *Biophys. J.* **2005**, *89*, 4006−4016.
(12) Pedersen, T. B.; Sabra, M. C.; Frokjaer, S.; Mouritsen, O. G.; Jørgensen. K. *Chem. Phys. Lipids* **2001**, *113*, 83−95.
(13) Silvius, J. R. In *Peptide−Lipid Interactions*; Simon, S. A., McIntosh, T. J., Eds.; Academic Press: San Diego, CA, 2002; pp 371−395.
(14) Malina, A.; Shai, Y. *Biophys. J.* **2005**, *89*, 4006−4016.
(15) Toniolo, C.; Crisma, M.; Formaggio, F.; Peggion, C.; Monaco, V.; Goulard, C.; Rebuffat, S.; Bodo, B. *J. Am. Chem. Soc*. **1996**, *118*, 4952−4958.
(16) Peggion, C.; Moretto, V.; Formaggio, F.; Crisma, M.; Toniolo, C.; Kamphuis, J.; Kaptein, B.; Broxterman, Q. B. *J. Pept. Res.* **2001**, *58*, 317−324.
(17) König, W.; Geiger, R. *Chem. Ber*. **1970**, *103*, 788−798.
(18) Carpino, L. *J. Am. Chem. Soc.* **1993**, *115*, 4397−4398.
(19) Didoné, M. Chemistry MSc thesis, University of Padova, Padova, Italy.
(20) Stewart, J. C. M. *Anal. Biochem.* **1980**, *104*, 10−14.
(21) Chen, R. F.; Knutson, J. R. *Anal. Biochem.* **1988**, *172*, 61−77.
(22) Chattopadhyay, A.; London, E.. *Biochemistry* **1987**, *26*, 39−45.
(23) Ladokhin, A. S.; Jayasinghe, S.; White, S. H. *Anal. Biochem.* **2000**, *285*, 235−245.
(24) Barret, D. A.; Hartshorne, M. S.; Hussain, M. A.; Shaw, P. N.; Davies, M. C. *Anal. Chem.* **2001**, *73*, 5232−5239.
(25) Murov, S. L.; Carmichael, I.; Gordon, L. H. *Handbook of Photochemistry*; Marcel Dekker: New York 1993; p 173.
(26) Beechem, J. M.; Gratton, E.; Ameloot, M.; Knutson, J. R.; Brand, L. In *Topics in Fluorescence Spectroscopy*; Lakowicz, J. R., Ed.; Plenum Press: New York, 1991; Vol. 2, pp 241−305.
(27) White S. H.; Wimley, W. C.; Ladokhin, A. S.; Hristova, K. *Methods Enzymol.* **1998**, *295*, 62−87.
(28) Rizzo, V.; Stankowski, S.; Schwarz, G. *Biochemistry* **1987**, *26*, 2751−2759.
(29) Schwarz, G. *Biophys. Chem.* **2000**, *86*, 119−29.
(30) Castanho, M.; Prieto, M. *Biophys. J.* **1995**, *69*, 155−168.
(31) Ladokhin, A. S. *Methods Enzymol.* **1997**, *278*, 462−473.
(32) London, E.; Ladokhin, A. S. In *Peptide−Lipid Interactions*; Simon, S. A., McIntosh, T. J., Eds.; Academic Press: San Diego, CA, 2002; pp 89−115.
(33) Chung, L. A.; Dear, J. D.; DeGrado, W. F. *Biochemistry* **1992**, *31*, 6608−6616.